



Research article

Development, characterization, and evaluation of Zn-SA-chitosan bionanoconjugates on wheat seed, experiencing chilling stress during germination

Narender Mohan ^{a, **}, Ajay Pal ^a, Vinod Saharan ^b, Anuj Kumar ^c, Rahul Vashishth ^{d, *}, Sabina Evan Prince ^e^a Department of Biochemistry, College of Basic Sciences and Humanities, Chaudhary Charan Singh Haryana Agricultural University, Hisar, Haryana, 125 004, India^b Department of Molecular Biology and Biotechnology, Rajasthan College of Agriculture, Maharana Pratap University of Agriculture and Technology, Udaipur, Rajasthan, 313 001, India^c ICAR- Indian Institute of Wheat and Barley Research, Karnal, Haryana, 132001, India^d Department of Biological Sciences, School of Bio Sciences and Technology, Vellore Institute of Technology, Vellore, 632014, India^e Department of Biotechnology, School of Bio Sciences and Technology, Vellore Institute of Technology, Vellore, 632014, India

ARTICLE INFO

Keywords:

Bionanoconjugate
Nanoprimering
Release kinetics
Seed reserve mobilization
Chilling stress
Vigour index

ABSTRACT

This study aimed to develop and characterize the chitosan bionanoconjugates (BNCs) loaded with zinc (Zn) and salicylic acid (SA) and test their efficacy on wheat seed exposed to chilling stress. BNCs developed were spherical (480 ± 6.0 nm), porous, and positively charged ($+25.2 \pm 2.4$ mV) with regulated nutrient release properties. They possessed complexation efficiency of 78.4 and 58.9 % for Zn, and SA respectively. BET analysis further confirmed a surface area of 12.04 m²/g. Release kinetics substantiated the release rates of Zn and SA, as 0.579 and 0.559 % per hour, along with a half-life of 119.7 and 124.0 h, respectively. BNCs positively affected the germination potential of wheat seeds under chilling stress as observed by significantly ($p < 0.05$) reduced mean emergence time (18 %), and increased germination rate (22 %), compared to the control. Higher activities of reserve mobilizing enzymes (α -amylase- 6.5 folds, protease –10.2 folds) as well as faster reserve mobilization of starch (64.4 %) and protein (63.5 %) molecules were also observed. The application further led to increased levels of the antioxidant enzymes (SOD and CAT) and reduced oxidative damage (MDA and H₂O₂). Thus, it is inferred that the developed BNCs could help substantially improve the germination and reserve mobilization potential, thereby increasing the crop yield.

1. Introduction

The global population is expanding alarmingly and is expected to reach 9 billion by 2050. A significant part (>50 %) of this population consumes wheat (*Triticum aestivum* L.), and it is anticipated that global wheat demand will increase by 70 % by 2050 [1]. Under global warming, wheat is one of the most affected crops and needs attention to sustain its productivity [2]. Late wheat planting

* Corresponding author.

** Corresponding author.

E-mail addresses: narendermohan93@gmail.com (N. Mohan), rahul.vashishth@vit.ac.in (R. Vashishth).

has become a frequent practice due to the delayed harvesting of prior crops like cotton, paddy, sugarcane, pigeon pea etc. Because of this, the wheat crop experiences cold stress during germination resulting in uneven stand establishment [3]. Chilling stress during seed germination in late-sown wheat later leads to terminal heat stress resulting in reduced growth and decreased yield. Therefore, it is imperative to enrich the novel research strategy desired to sustain wheat productivity in a changing environment to fulfill the rising food demand [4]. Unique and alternative techniques viz., increasing the seed's germination potential, improving the signalling network, and finally resulting in crop establishment and production must be devised to combat multi-dynamic environmental changes [5]. In this scenario, seed priming was introduced in crops for (i) homogenous and higher germination potential, (ii) better mobilization of seed reserves, (iii) enhanced signalling network resulting in the better establishment of a plant to cope with environmental stress [6,7]. Seed priming activates 'pre-germinative metabolism' that affects germination and emergence, allowing seeds to withstand harsh conditions [8]. To date, various priming techniques and solutions like water (hydropriming), polyethylene glycol and inorganic salts (osmopriming), hormonal priming (IAA, GA₃, SA, etc.) and nutrient priming (Fe, Cu, Se, Zn, etc.) are commonly used [9,10].

Zinc (Zn) is recognized as a critical micronutrient and a component of over 300 plant enzymes and vital proteins in plants [11]. Earlier studies show that compared to unprimed seeds, priming with Zn increased SVI-1 and SVI-2 by 94 and 77 %, respectively, resulting in improved seedling development and yield [12]. Zinc oxide and zinc sulfates are commonly used as zinc fertilizers to ameliorate Zn deficiency in plants. However, their applications as fertilizer are restricted because of their low solubility and availability [13]. Salicylic acid (SA), an endogenous growth regulator, is a crucial phenolic compound with low solubility in water (0.011 M at 20 °C) that affects plant growth and development by participating in signalling and physiological processes. Its exogenous application as seed treatment and foliar application induces many metabolic processes in plants and can be an alternative approach for controlling disease and enhancing plant growth and yield [14]. It stimulates seed germination and root growth and improves seedling stress tolerance. However, SA has low water solubility and is prone to environmental degradation factors such as light, air, and temperature; therefore, it will be more biologically active if protected/encapsulated.

The priming techniques use excess nutrients that can be toxic to plant health (immediate high concentration) and soil (leached-out nutrients). In this case, large amounts of the nutrients are washed off (not in plant use), so sustained-release fertilizer is needed. The synchronized release of essential micronutrients and hormones via nanoparticles could be a superior approach for meeting the germinating requirements [15]. It is emerging as a promising method because it provides advanced and alternate ways of exogenous applications of biopolymers, micronutrients, and plant growth hormones to enable higher seed germination and plant production [16, 17].

Many biopolymers, such as alginate, starch, cellulose, chitin, and chitosan, have recently been used to generate novel materials that aid crop growth and protection [18]. However, the sustainability of agriculture has recently been credited to chitosan and its derivatives, which are readily available and packed with several advantages. Chitosan is the second most abundant biopolymer after cellulose. It is a non-toxic, biodegradable, and biocompatible substance that reduces the adverse effects of stresses, upgrades the defense system, and enhances plant growth by increasing the availability and uptake of water and essential nutrients [19]. Chitosan is widely employed as a nano-chitosan and nanocarrier by encapsulating active molecules (metals, hormones, etc.) [20,21]. It also acts as a good nitrogen source for plants as its main component comprises nitrogen absorbed by the plants.

Nano-chitosan fortification with essential nutrients is more valuable than pure/bulk chitosan [19,22] and the application of chitosan nanocomposites containing some valuable components (Zn, Cu, Fe, and SA) to improve the physio-biological activities for better results [23–26] has been conducted. Sufficient literature with the sole benefits of these molecules in their bulk and nanoforms is available, showing improved crop growth, productivity, and yield. However, cumulative studies of these molecules entrapped in one nanoconjugate system and their application to plant physiological and biochemical mechanisms involved during seed germination have not been elucidated. Thus, the present investigation aimed to synthesize and characterize the bionanoconjugates (formulation encapsulating both Zn and SA as a single conjugate), and test their efficacy to improve seed germination potential, reserve mobilization and antioxidative system in wheat under chilling stress during germination.

2. Materials and methods

Chitosan (mol. wt. 50–190 kDa; N-deacetylation >85 %) and sodium tripolyphosphate (TPP) were purchased from Sigma-Aldrich (St. Louis, USA). Reagents for biochemical and other assays were purchased from HiMedia and SRL (Mumbai, India). Seeds of wheat variety WH-1124 were obtained from the Wheat and Barley Section, Department of Genetics and Plant Breeding, CCS Haryana Agricultural University, Hisar.

2.1. Preparation of Zn-SA-chitosan BNCs

The ionotropic gelation process was used to develop Zn-SA-chitosan BNCs with certain modifications [27]. Chitosan was dissolved in 1.0 % (v/v) acetic acid and continuously stirred until a clear solution was formed. Cross-linking was achieved by adding TPP (cross-linker) to the chitosan solution in a dropwise manner and stirring continuously. ZnSO₄ (0.15 %) and SA (0.1 %) were sequentially added to the colloidal solution during cross-linking. The reaction mixture (RM) was sonicated three times (pulse rate: 9 s on - 5 s off, frequency- 50 %; power- 500 W) followed by centrifugation at 12,000 rpm under dust-free conditions to obtain the pellets of Zn-SA-chitosan BNCs. The pellets were lyophilized and stored at room temperature until further use.

2.2. Physico-chemical characterization of Zn-SA-chitosan BNCs

2.2.1. DLS and zeta-potential

Particle size, polydispersity index (PDI) and zeta-potential of synthesized BNCs were measured using dynamic light scattering (Malvern- MAL1265866, version: 2.1.0.15) with an appropriate sample loading index. Three batch samples were dissolved in deionized water (10 mg/20 ml), then examined at 25 °C with a scattering angle of 90° and a detector angle of 173° (backscatter) using 45 runs per sample [28].

2.2.2. TEM, SEM, and EDS analyses

Samples were prepared for Transmission Electron Microscopy (TEM) by pouring 25 µl of sonicated BNCs solution onto the grid (400-mesh Form var carbon-coated zinc grid), wicking out the surplus sample with filter paper after 35 s, and drying it. The Zn-SA-chitosan BNCs were TEM micro-graphed using an FEI Spirit TEM (Hillsboro, USA) with an accelerating voltage of 0.1 kV [29,30]. However, the Zn-SA-chitosan BNCs were dried by critical point drying (CPD, Emitech K850) and sputter-coated with gold-palladium (SC7620, Emitech) after mounting on aluminum stubs containing double-sided carbon and SEM micrographs were taken with a Zeiss EVO MA10 SEM (Carl Zeiss Promenade, Jena, Germany) in high vacuum mode at 15 kV EHT (Extra high tension) at 400× and 29.70× magnifications. Further, the purity, chemical composition and elemental analysis of a dried sample of BNCs were studied by an Energy Dispersive X-ray Spectroscopy (EDS) analyser (Bruker XFlash 6130) [31].

2.3. Physisorption technique for surface study

2.3.1. BET and isotherm analysis

The Brunauer Emmett Teller (BET) analysis was performed at 77.35 K using Quantachrome® ASiQwin™ 1994-2017, Quantachrome Instrument v5.21. Outgassing was carried out in a 6 mm cell type containing the sample adsorbed by nitrogen at 120 °C for 8.3 h. The sample was then used to conduct surface investigations, including specific surface area (m²/g), pore radius, volume, size, cumulative pore surface area, and pore width at a particular relative pressure (P/P₀) [32].

2.4. Chemical analytical techniques (spectroscopy)

2.4.1. FTIR (Fourier transform infrared spectroscopy)

FTIR spectrometer was used to gaze at the functional groups and bond interaction in Zn-SA-chitosan BNCs (PerkinElmer Spectrum IR Version 10.7.2). Freeze-dried BNCs (1 part) were gently pestled with KBr (99 parts) and scanned against a blank KBr pellet background. Fifty-two scans in the wavelength range of 400–4000 cm⁻¹ were used to record the spectra of the samples [33].

2.4.2. Inductively coupled plasma-mass spectrometry (ICP-MS) and UV-Vis spectroscopy

The complexation efficiency (CE), yield potential (YP), loading capacity (LC), and *in vitro* release profile of Zn and SA were determined using ICP-MS and UV-Vis spectroscopy. Known amounts of synthesized BNCs were dispersed in deionized water at room temperature in two sets of ten tubes, one set for Zn and the other for SA. After every 24 h, aliquots from each tube were collected to estimate Zn and SA using the appropriate methods [34]. The *in vitro* release of the Zn and SA at various intervals was studied after dispersing the BNCs in pH adjusted (1–7) deionized water. For Zn estimation, collected samples were digested (appropriate mixture of nitric acid and H₂O₂ for 90 min at 180 °C), diluted to a suitable concentration, and filtered with syringe filters before loading. The samples were analyzed using the KED (Kinetic energy discrimination) technique in an ICP-MS (ThermoFisher Scientific, model no. i-CAP RQ) [34].

The CE, YP and LC were calculated as follows:

$$CE (\%) = \frac{\text{Total amount of Zn or SA added in the RM} - \text{Zn or SA in supernatant}}{\text{Total amount of Zn or SA added in the RM}} * 100 \quad (1)$$

$$YP (\%) = \frac{\text{Weight of lyophilized BNCs}}{\text{Weight of components contained in the RM}} * 100 \quad (2)$$

$$LC (\%) = \frac{\text{Weight of Zn or SA in BNCs}}{\text{Weight of BNCs}} * 100 \quad (3)$$

2.4.3. Release kinetics

The results of the Zn and SA release profiles were expressed as first-order release rate constants (K_r) using the equation [35]:

$$\ln \frac{A}{A_0} = -K_r T \quad (4)$$

where, A is residual Zinc/SA; A₀ is the total Zinc/SA; K_r is the release rate constant, and T is the time of release.

Half-life (T_{1/2}) and decimal reduction value (D-value) of the complexed Zinc and SA were computed using the equations:

$$T_{\frac{1}{2}} = \frac{\ln 2}{K_r} \quad (5)$$

$$D \text{ value} = \frac{\ln 10}{K_r} \quad (6)$$

2.5. In vitro seedling experiment

Wheat seeds were surface-sterilized with 2 % sodium hypochlorite for 10 min and primed with different concentrations of BNCs for 12 h in a beaker [7]. The primed seeds were divided into two groups and then a part of the primed seeds was transferred on the petri plates lined with the germination paper and the remaining were placed onto germination paper layered with another sheet of paper. These layered papers are folded so that the base of the papers was immersed in the water contained within the beaker. The first part hydro-conditioned (5.0 ml) regularly and placed in a growth chamber at 10 ± 1 °C (cold stress conditions).

α -Amylase, protease, starch and protein were estimated at 0, 1, 3, 5, 7 and 9 days after germination (DAG) [36]. The α -amylase activity (unit/g Fwt) was measured following the standard protocol [37], where one unit is defined as μ mole of substrate utilized per min. For protease activity (unit/g Fwt), the germinating seeds were homogenized in phosphate buffer (pH 7.6) at 4 °C and enzyme action was initiated at 37 °C upon adding casein (1 % w/v) as a substrate. After 20 min, 10 % trichloroacetic acid (TCA) was added to precipitate the proteins and cease the reaction. The precipitates were removed, and the supernatant was allowed to react with alkaline copper reagent at room temperature (10 min) followed by Folin Ciocalteu reagent (FCR) input. The mixture was incubated in the dark (30 min) at room temp and absorbance was recorded at 620 nm. One unit corresponds to μ mole/min. Similarly, starch and protein contents were estimated at regular intervals following the standard methods, respectively [38,39].

Chlorophyll and carotenoids were quantified in fresh leaf tissue at 15thDAG to assess the effects of BNCs on the photosynthetic potential of seedlings [40]. Similarly, stress indicators (MDA and H₂O₂) and antioxidant enzyme (catalase) were also estimated on 15th DAG in seedling leaves. MDA was estimated [41] using fresh tissue (200 mg) homogenized in 2.0 ml of 0.1 % trichloroacetic acid and centrifuged at 8000 rpm for 15 min. The supernatant (0.5 ml) was added to 2.3 ml of 20 % TCA containing 0.5 % thiobarbituric acid. After boiling the mixture in a water bath for 30 min, it was quickly cooled in an ice bath. The absorbance was recorded at 532 nm, and the non-specific absorbance value at 600 nm was subtracted. MDA content was calculated using the molar extinction coefficient ($155 \text{ mM}^{-1} \text{ cm}^{-1}$). In the case of hydrogen peroxide [42], sample (200 mg) was macerated in 2.0 ml of ice-cold 0.01 M phosphate buffer (pH-7.0), and the supernatant was collected after centrifugation (10,000 rpm for 10 min). 0.6 ml of 0.1 M phosphate buffer (pH 7.0) and a 3.0 ml mixture of 5 % (w/v) potassium dichromate and glacial acetic acid (1:3, v/v) were added to the 0.4 ml extract and boiled (10 min) until the formation of the formation of green colored chromic acetate. The content was cooled, and the absorbance was recorded at 570 nm against the reagent blank without sample extract. The quantity of H₂O₂ was determined using the standard curve of H₂O₂.

For catalase assay [42], a leaf sample (200 mg) was crushed in 2 ml of 0.1 M phosphate buffer (pH 7.0) containing 1.0 % PVP and the homogenate was centrifuged at $10,000 \times g$ for 20 min in a refrigerated centrifuge at 4 °C. A reaction mixture containing 0.5 ml 0.1 M phosphate buffer (pH 7.5), 0.4 ml 0.2 M H₂O₂ and 0.1 ml supernatant was incubated at 37 °C. The reaction was terminated by adding 3 ml potassium dichromate reagent and the reaction mixture was then boiled for 10 min. The absorbance at 570 nm was measured using



Fig. 1. Priming experiments in the laboratory under controlled conditions showing growth in primed seeds (T1-control, T2-bulk chitosan, T3-bulk Zn, T4-bulk SA, T5- Mix bulk (chitosan, Zn and SA), T6-0.1 %, T7-0.2 %, T8-0.4 %, T9-0.8 %, T10-1.2 %, T11-1.6 % BNCs.

the potassium dichromate reagent as a blank. An assay mixture devoid of enzyme extract was used as a control. The absorbance of the sample was subtracted from the control to estimate the residual amount of H₂O₂ in the mixture. One enzyme unit was defined as the amount of enzyme required to catalyze the oxidation of 1.0 μmole of H₂O₂ in 1 min under given assay conditions. In the supernatant obtained above, the superoxide dismutase activity was determined by the rate of inhibition of nitroblue tetrazolium by photochemical reduction. The reaction was monitored at 560 nm. One unit of SOD is defined as the amount of enzyme required to cause 50 % inhibition [43].

To the other group (ii.) of primed seeds, the between-paper approach was employed to analyze the root-shoot length, root number, and seedling lengths at regular intervals (Fig. 1). On the 15th day, the seedlings' fresh and dried weights were measured. The experiment followed the International Seed Testing Association's guidelines [16]. The following formulae were used to compute the seed vigour index (SVI- I and II), germination rate (GR), mean emergence time (MET) and coefficient of germination (COG):

$$SVI-1 = \text{Germination \%} \times \text{seedling length [44] (Equation-7)}$$

$$SVI-2 = \text{Germination \%} \times \text{seedling dry weight [44] (Equation-8)}$$

$$GR = \frac{G1}{T1} + \frac{G2}{T2} + \dots + \frac{Gn}{Tn} * 10 \tag{9}$$

$$MET = \frac{\sum ni * di}{N} \tag{10}$$

$$COG = \frac{100(A1 + A2 + \dots + An)}{A1T1 + A2T2 + \dots + AnTn} \tag{11}$$

where,

G1 = No. of seedlings emerged on 1st day; G2 = No. of seedlings emerged on 2nd day; Gn = No. of seedlings emerged on nth day; T = Days to germination; N = total number of seeds; ni = germinated seeds on the counting day; di = counting day.

2.6. Statistical analysis

SPSS, the statistical analysis tool, was used to analyze the results to conclude the findings. These findings are presented in graphical and tabular form at a significance level of $p = 0.05$.

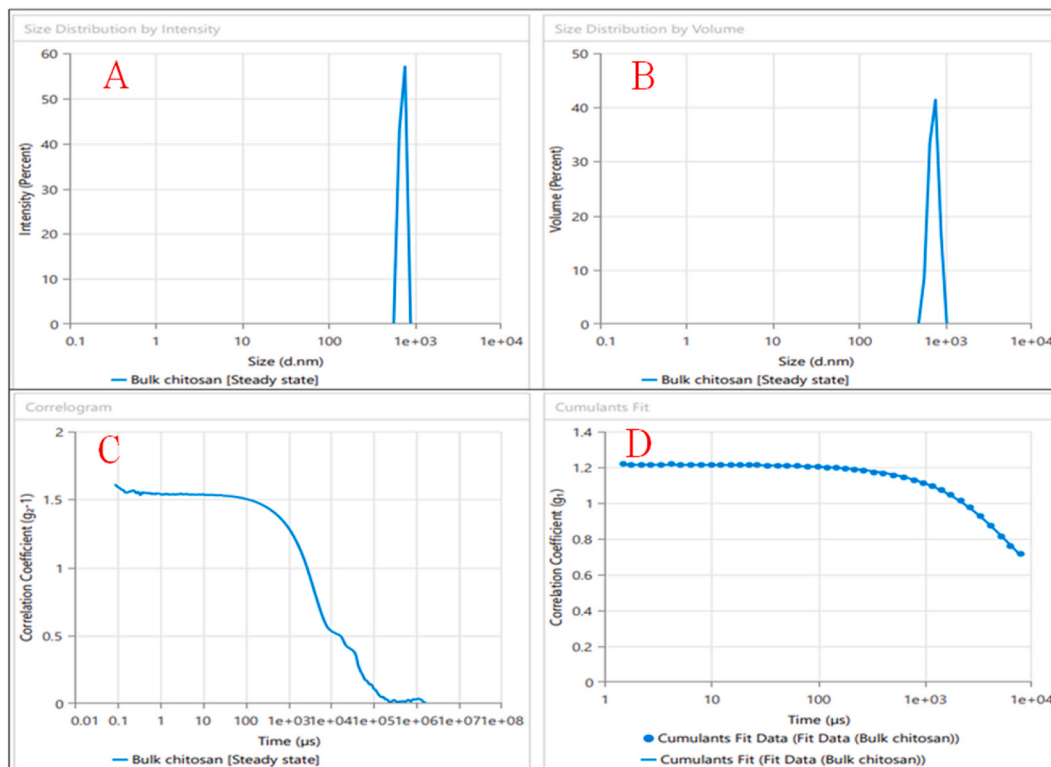


Fig. 2. Particle size distribution based on intensity (A) and volume % (B) of bulk chitosan and their correlogram (C) and cumulants fit (D) based on correlation coefficient vs time.

3. Results

3.1. Synthesis, yield and DLS results of engineered Zn-SA-chitosan BNCs

The ionic interactions of TPP (negatively charged cross-linker) and chitosan (positively charged backbone) encapsulating Zn and SA resulted in Zn-SA-chitosan BNCs with a hydrodynamic diameter of 480–520 nm (Fig. 3). The DLS study, along with size, also revealed that the zeta-potential of these BNCs was +22.7–27.6 mV, with a PDI of 0.18–0.24 (Fig. 3a and b). Moreover, the graphs of correlogram (Figs. 2c and 3c) and cumulants (Figs. 2d and 3d) fit based on correlation coefficient vs time additionally supports the lower dispersity of BNCs compared to bulk chitosan having more area under the curve than BNCs. Bulk chitosan had particle size >2600 nm and greater PDI (>0.8) and zeta-potential (+42–52 mV) (Fig. 2a and b). A 500 ml reaction volume (having chitosan 1 g, TPP 0.4 g, ZnSO₄ 0.1 g and SA 0.08 g) yielded approximately ~0.8 g of dull white crystalline powder.

3.1.1. SEM, TEM, and EDS studies

The SEM micrograph revealed the presence of pores in the developed BNCs (Fig. 4a) while the TEM study revealed that Zn-SA chitosan nanoconjugates composed of aggregated spherical-shaped nanoparticles (inset, Fig. 4b). EDS study showed the presence of C (42.72 wt%), O (44.98 wt%), N (7.40 wt%), P (4.89 wt%) and Zn (0.01 %) in the nanocomposite (Fig. 5b). The findings of EDS also verify and demonstrate Zn's imprisoned companionship in the BNCs (Fig. 5a).

3.1.2. FTIR studies

The FTIR spectra mapped the peaks related to -NH₂ (1° amine) and -OH at 3400 cm⁻¹, CO-NH₂ (amide) at 1650 cm⁻¹ and the anhydrous glycosidic peak of bulk chitosan at 896 cm⁻¹. The spectrum presents a peak transfer from 3400 to 3452 cm⁻¹ corresponding to amalgamated peaks of NH₂ and OH group of chitosan due to stretching vibration. The cross-linking of Zn, TPP, and amino groups of chitosan is shown by a peak shift from 1650 to 1594 to 1642 and 1560 cm⁻¹, respectively, in SA-Zn chitosan BNCs (Fig. 6). A considerable shift from lower to higher wave number (1073–1085 cm⁻¹) in SA-Zn chitosan BNCs indicates the participation of the OH group of chitosan.

The peaks representing the acetoxy group of SA, previously mapped at 1542 and 1647 cm⁻¹, were reallocated to 1539 and 1641 cm⁻¹ (Fig. 6). Interaction of -COOH group in SA with 1° amine of chitosan was recasted to 1311 cm⁻¹ in BNCs. A hypothetical model based on FTIR mapping that reveals the interactions of Zn, SA, TPP, and chitosan in the developed BNCs is shown in Fig. 7.

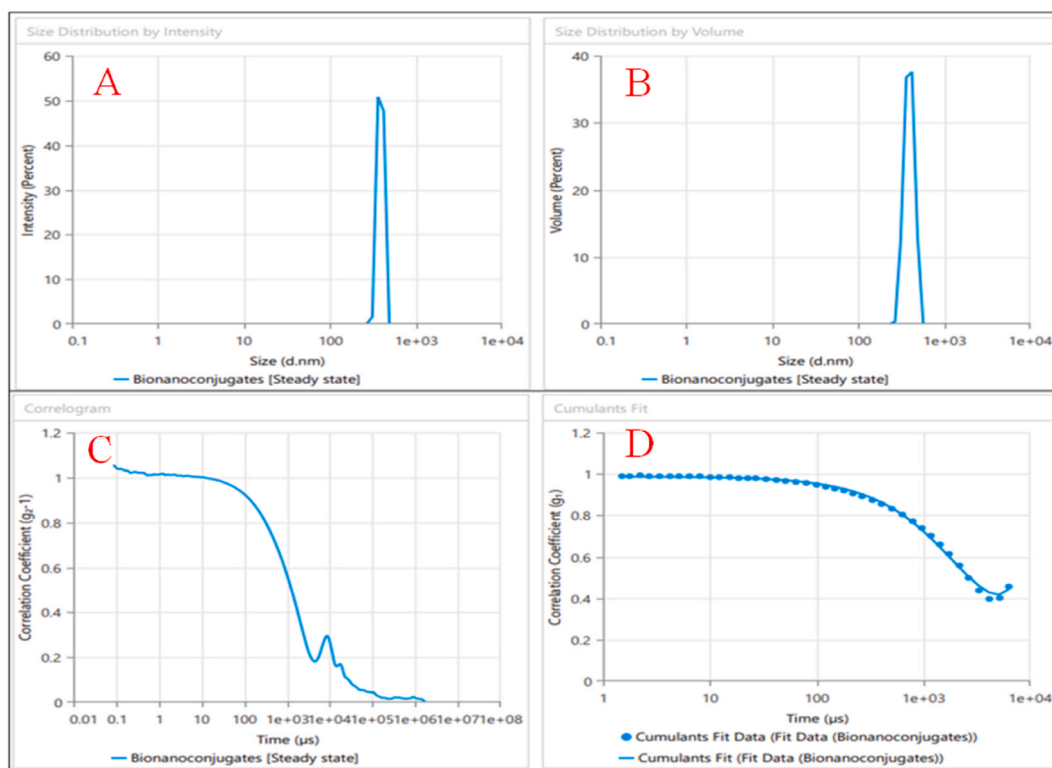


Fig. 3. Particle size distribution based on intensity (A) and volume % (B) of synthesized BNCs and their correlogram (C) and cumulants fit (D) based on correlation coefficient vs time.

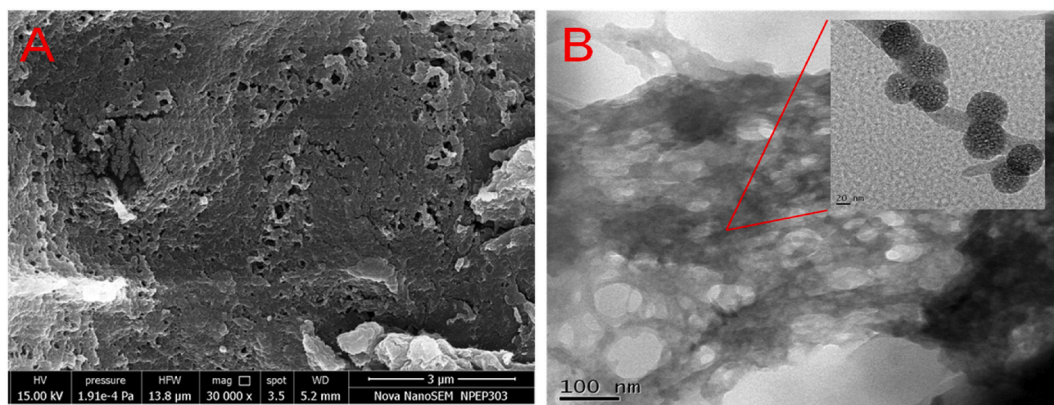


Fig. 4. SEM (A) micrographs at 30kx showing porous surfaced Zn-SA chitosan BNCs and TEM (B) micrograph entails spherical shaped aggregated (at 200kx) and dispersed NPs in the inset.

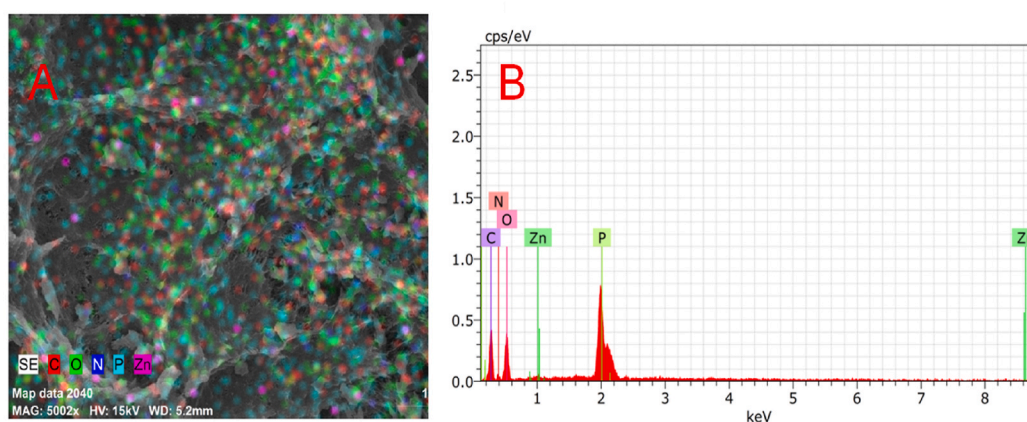


Fig. 5. EDS analysis of Zn-SA chitosan BNCs (A) mapping of elements and (B) elemental composition.

3.1.3. BET and isotherm

The detailed description of the surface area ($1.690 \text{ m}^2/\text{g}$), pore volume (0.015 cc/g) and pore radius (21.543 \AA) of bulk chitosan are shown in Table 1. The BJH desorption report for BNCs showed a $12.04 \text{ m}^2/\text{g}$ surface area, 0.171 cc/g pore volume, and a 19.117 \AA pore radius (Table 1).

3.1.4. Complexation efficiency (CE), loading capacity (LC), and yield potential (YP) and in vitro release profile

In the present study, the CE and LC of Zn-SA-chitosan BNCs were remarkable, with CE and LC values for Zn being 78.4 and 2.19 % and for SA being 58.9 and 5.8 %, respectively. The reaction mixture's yield potential was found to be 52.7 %.

In-vitro release studies were conducted to calculate the release and retention percentages of Zn and SA (Figs. 8–10). Due to the protonation of the amino group of chitosan at low pH, a quicker release at this pH was seen in the pH-dependent release profile (pH range 1.0–7.0). At pH 1.0, it was found that 88.9 % of the Zn (Fig. 8a) and 79.8 % of the SA (Fig. 8b) were released within 24 h, compared to 31.8 and 16.4 %, respectively, at neutral pH (Fig. 8). The time-dependent release profile showed that 32 % and 16 % of Zn (Fig. 9a) and SA (Fig. 9b) were released at 24 h (pH-7). Furthermore, 80 % and 74 % of Zn and SA were progressively released at 240 h (Fig. 9).

3.1.5. Kinetics of release

First-order kinetics was used to calculate the release rate constants (K_r) for Zn (Fig. 10a) and SA (Fig. 10b), which were found to be 0.00579 and 0.00559 h^{-1} , respectively (Fig. 10). It shows that entrapped Zn and SA are released at rates of 0.579 and 0.559 % per hour, respectively. The Zn and SA releases had a half-life ($T_{1/2}$) of 119.7 and 124.0 h and a 90 % release time of 397.7 and 411.9 h, respectively.

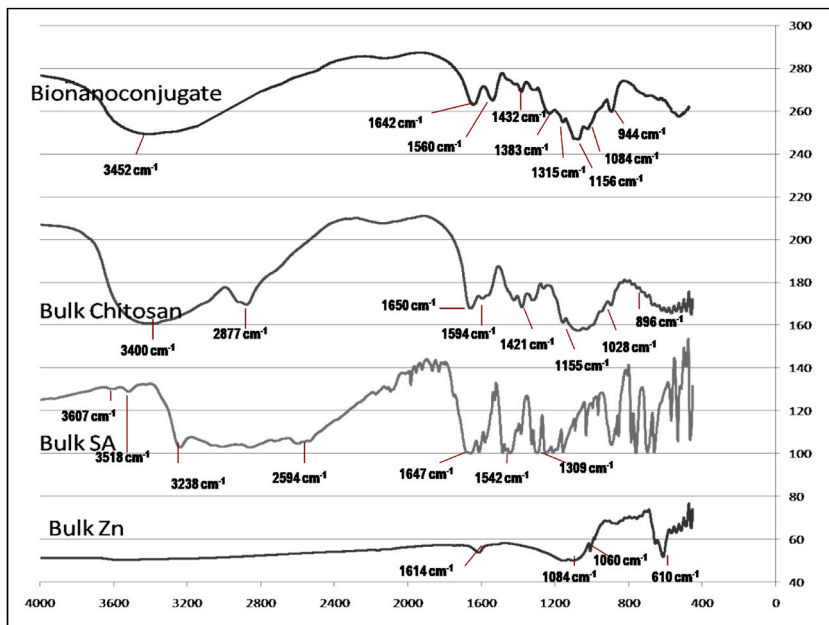


Fig:6. Comparative FTIR results of bulk chitosan and Zn-SA-chitosan BNCs.

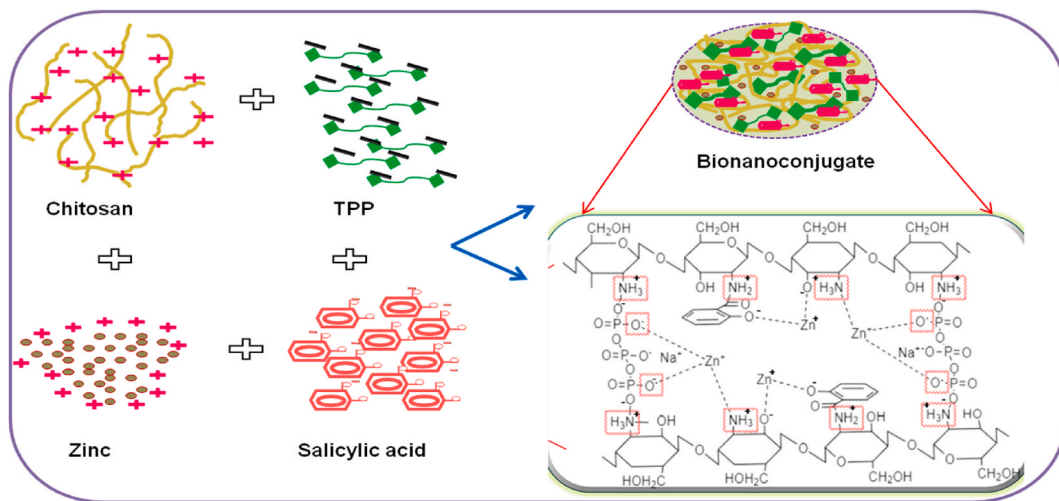


Fig: 7. Speculative morphology of Zn-SA-chitosan BNCs: Blending bulk Zn, SA, chitosan and TPP forming a nanostructure possessing backbone of chitosan cross-linked by TPP encapsulating Zn and SA.

Table 1
BJH desorption summary of both bulk chitosan and Zn-SA-Chitosan BNCs.

Properties	Bulk chitosan	BNCs	Units
Surface area	1.690	12.049	m ² /g
Pore volume	0.015	0.171	cc/g
Pore Radius D _v (r)	21.543	19.117	Å

3.2. In vitro seed and seedling analyses

The impact of Zn-SA-chitosan BNCs on wheat seedling growth parameters is shown in Table 2. All the parameters were reported on the 10th DAG in petri plates shown in Table 2. Very low germination was reported in all treatments for 0–3 days. On the 10th day after

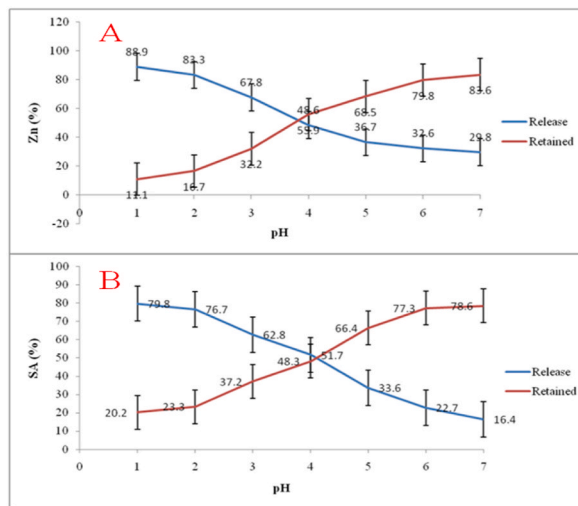


Fig. 8. - Release and retention profile of Zn (A) and SA (B) at varying pH (1–7).

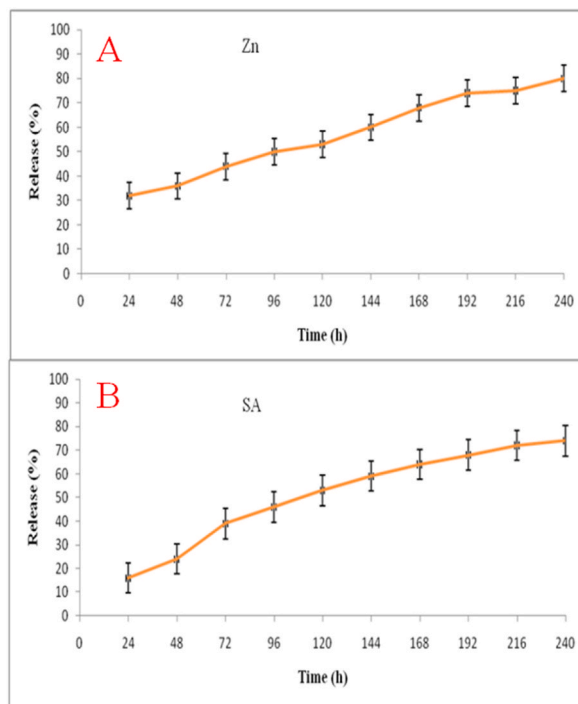


Fig.9. Release profile of Zn (A) and SA (B) at various incubation times.

germination (DAG), BNCs-primed seeds (0.1–1.6 %) showed a significant difference in germination rate, coefficient of germination, and germination percent (Table 2). An increase in germination rate when seeds were treated with 0.4 % BNCs was 22 % higher than the control. Moreover, the mean emergence time recorded in control was 7.3 days, whereas 0.4 % BNCs reduced the emergence time to 5.9 days. BNCs (0.4 %) treatment showed faster emergence of up to 18 % compared to the control (Table 3). However, a significant change was not observed within the BNCs treated plants after 0.4 %.

Characters like root-shoot length, seedling length, fresh and dry weight recorded in Table 3 were observed at 15th DAG on germination paper. The maximum increase in shoot and root lengths were observed in 0.4 % BNCs-treated seeds. The growth of the seedlings in WH-1124 was observed to be enhanced in all treatments. When treated with BNCs, a maximum dry weight of 0.118 g was recorded in 0.4 % and 1.2 %. Similarly, fresh weight was found maximum in 0.4 % (1.25 g) followed by 0.8 % (1.24 g). Both mixed bulk and bulk chitosan showed no signs of germination; thus, the treatments are absent in Tables 2 and 3. But seedling length significantly

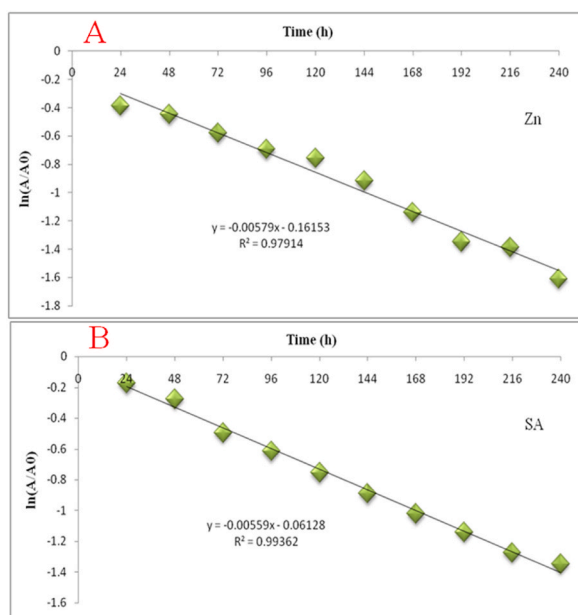


Fig. 10. Release kinetics of Zn (A) and SA (B).

Table 2

Effect of seed treatment by BNCs on germination potential determining traits [Germination rate (G. rate), coefficient of germination (COG), germination percent (Ger. %), Seed vigour index (SVI-I and II)].

Treatment	G. rate	COG	Ger. %	SVI-I	SVI-II
Control	6.84 ± 0.03	12.8 ± 0.05	100 ± 1.1	927 ± 60.1	6.3 ± 0.89
Bulk Zn (0.1 %)	7.08 ± 0.15	13.1 ± 0.06	100 ± 0.9	1068 ± 37.6	7.6 ± 0.78
Bulk SA (0.1 %)	6.96 ± 0.11	13.0 ± 0.06	96.7 ± 0.9	1047 ± 33.3	7.8 ± 1.02
BNCs					
0.1 %	7.83 ± 0.15	13.2 ± 0.03	100 ± 1.7	1283 ± 106.2	10.4 ± 0.68
0.2 %	7.95 ± 0.06	13.3 ± 0.05	100 ± 0.9	1504 ± 91.7	11.0 ± 0.53
0.4 %	8.38 ± 0.07	13.4 ± 0.07	100 ± 0.8	1607 ± 55.1	11.6 ± 2.01
0.8 %	8.31 ± 0.15	13.5 ± 0.09	96.7 ± 0.9	1591 ± 37.6	11.4 ± 1.03
1.2 %	8.30 ± 0.08	13.5 ± 0.04	100 ± 1.9	1565 ± 37.1	11.3 ± 1.11
1.6 %	8.05 ± 0.02	13.5 ± 0.06	96.7 ± 1.2	1581 ± 108.6	11.3 ± 2.84

CD at 5 % (p = 0.05) G. rate – 0.108, COG – 0.073, Ger. % – 0.5.

Table 3

Effect of seed treatment by BNCs on seedling characteristics [mean emergence time (MET), shoot length (SL), root length (RL), seedling length (Seedling L.), seedling fresh weight (Seedling Fwt.) (g), seedling dry weight (Seedling Dwt.) (g)].

Treatment	MET	SL	RL	Seedling L (cm)	Seedling Fwt. (g)	Seedling Dwt. (g)
Control	7.3 ± 0.21	4.9 ± 0.3	5.7 ± 0.51	10.5 ± 0.3	0.76 ± 0.039	0.072 ± 0.07
Bulk Zn (0.1 %)	7.0 ± 0.14	5.2 ± 0.4	6.7 ± 0.41	11.9 ± 1.3	0.89 ± 0.081	0.084 ± 0.004
Bulk SA (0.1 %)	7.1 ± 0.22	5.3 ± 0.5	6.6 ± 0.58	11.9 ± 0.2	0.92 ± 0.102	0.089 ± 0.009
BNCs						
0.1 %	6.3 ± 0.18	5.7 ± 0.4	7.8 ± 0.21	13.5 ± 1.2	1.10 ± 0.106	0.109 ± 0.006
0.2 %	6.2 ± 0.09	7.3 ± 0.2	8.2 ± 0.36	15.5 ± 0.4	1.18 ± 0.141	0.113 ± 0.010
0.4 %	5.9 ± 0.19	7.8 ± 0.5	8.8 ± 0.53	16.4 ± 0.4	1.25 ± 0.163	0.118 ± 0.008
0.8 %	7.3 ± 0.23	4.9 ± 0.3	5.7 ± 0.51	10.5 ± 0.3	0.76 ± 0.039	0.072 ± 0.07
1.2 %	7.0 ± 0.26	5.2 ± 0.4	6.7 ± 0.41	11.9 ± 1.3	0.89 ± 0.081	0.084 ± 0.004
1.6 %	7.1 ± 0.18	5.3 ± 0.5	6.6 ± 0.58	11.9 ± 0.2	0.92 ± 0.102	0.089 ± 0.009

CD at 5 % (p = 0.05)SL – 0.687, RL – 0.731, Seedling L – 1.023, S. Fwt. – 0.061, S. Dwt. – 0.008.

improved when Zn, SA, and BNCs (0.1–1.6 %) treatments were compared to the control.

Seeds treated with BNCs of 0.4 and 0.8 % concentration had a maximum seedling length of 16.4 cm. On the 15th DAG, it was discovered that the shoot-root, seedling length, and fresh and dry weights in BNCs treated seeds were considerably higher than the

control (Table 3). Seeds treated with 0.4 % BNCs produced better SVI-I (73 %) and SVI-II (82 %) results than the control, while the improvements were just 15 and 19 % for bulk zinc and almost 13 and 23 % for bulk SA, respectively. The increase in germination rate in nanoprimered (0.4 %) seeds was 8.15 ± 0.07 ; in control, it was recorded at 6.84 ± 0.03 . Similarly, the germination rate in bulk Zn and SA recorded was 7.08 ± 0.15 and 6.96 ± 0.11 , respectively. Additionally, a significant difference in the coefficient of germination between control (12.8) and nanoprimered (13.6) seeds was seen in 0.4 % BNCs treated wheat seeds. However, no germination was found in bulk chitosan and mixed bulk-treated seeds.

3.2.1. α -Amylase and protease activity

In the present study, we found that α -amylase activity changed when wheat seeds were primed with BNCs, as seen in Fig. 11a. It was observed that all the treatments had very minimal amylase activity on the 0th day of the experiment. At a later stage, α -amylase activity significantly increased in seeds treated with BNCs compared to bulk and control during 0th to 5th DAG. At 5th DAG, its activity in control seeds grew by 3.4 times, but in 0.4 % BNCs-treated seeds, it increased by 6.5 times (Fig. 11a). In comparison, bulk Zn and SA experienced a 4.8 and 5.8 fold increase from 0th to 5th DAG. The highest activity increase of 461 % from the 0th to 5th DAG was noted in 0.4 % BNCs treatment, whereas the increase in control was 328 % only on the 5th DAG. However, the activity decreased on subsequent days of germination as recorded up to the 9th DAG (Fig. 11a).

In 0.8 % treated seeds of wheat (WH-1124), protease activity increased 10.2 times, whereas it increased 5.3 times in control seeds from the 0th day to the 5th day after germination. Although the bulk Zn (6.4 folds) and SA (7.7 folds) treated seeds showed better results than the control, the activity increase was significantly lower than BNCs, showing a maximum increase on the 5th DAG compared to the control (Fig. 11b). The seeds treated with 0.8 % BNCs in WH-1124 had the maximum enzyme activity, whereas seeds treated with water had the lowest enzyme activity from 0th to 7th DAG. However, on the 9th day, the activity in BNCs-treated seeds was lowered, whereas the control exhibited higher activity than the treated seeds (Fig. 11b).

3.2.2. Protein and starch content

Seed food reserve, viz. starch and protein, decreased during germination, corresponding to the enzyme activity (α -amylase and protease). From 0th to 9th DAG, the bulk Zn and SA exhibited a moderate reduction of 5.1 and 4.6 mg g⁻¹ fwt, respectively, whereas 0.8 % BNCs experienced the largest loss of 6.46 mg g⁻¹ fwt. The control group had the highest leftover protein level, 5.78 mg g⁻¹ fwt (Fig. 11d). On the 9th day, protein reserve mobilization was quicker and more than 60 % protein was mobilized in BNCs treated seeds. However, only 42 % of reserve protein was mobilized in control. In contrast, the bulk Zn and SA showed up to 51 and 45 % reserve protein mobilized on the 9th DAG (Fig. 11d).

A similar trend in starch content was reported, as seen in protein. On the 9th day, the BNCs-treated seeds utilized more than 60 % of the reserved starch with maximum utilization of 0.8 % (64.44), followed by 1.2 and 1.6 % (64.34 %), 0.4 % (63.9 %), and least in the 0.1 % (60.1 %). Maximum utilization in bulk was recorded in Zn (54.60 %) treated plants compared to minimal starch utilization in bulk SA (52.56 %). The minimum starch was mobilized in the control seeds with only 44.82 % mobilization on the 9th DAG (Fig. 11c).

3.2.3. Chlorophyll and carotenoid content

Chlorophyll *a*, *b*, and total chlorophyll content changed in WH-1124 after BNCs treatment (Fig. 12a). Results show that 0.4 % BNCs-treated seeds had the maximum total chlorophyll content (5.34 mg g⁻¹ fwt), while control seeds had the lowest (3.09 mg g⁻¹ fwt). Whereas, in bulk Zn and SA, the seeds treated had a total chlorophyll content of 3.78 and 4.18 mg g⁻¹ fwt, respectively (Fig. 12a). Moreover, on BNCs treatment (0.4 %), the increase observed in chlorophyll *a* and *b* was 54.4 and 124.9 % higher than in control. In bulk Zn, the increase in chlorophyll *a* and *b* was only 30.7 and 47.4 %, respectively, compared to the control. Moreover, chlorophyll *a* and *b* in SA increased by 42.8 and 54.7 %, respectively. Additionally, the chlorophyll *a* and *b* ratio observed was altered from 1:2.86 in control to 1:2 in BNCs (0.4 %) treated plants (Fig. 12a). It was also recorded that when seedlings were treated with BNCs instead of controls, their carotenoid content increased significantly during germination. The 0.4 % had the highest carotenoid content (0.9 mg g⁻¹) compared to the control having the values of 0.5 mg g⁻¹ fwt, respectively (Fig. 12b).

3.2.4. Stress indicators content

To assess the effects of BNC and chilling stress, we measured the content of MDA and H₂O₂. MDA content declined in BNCs-treated seeds by 39 % compared to the control (Fig. 13b). Bulk Zn and SA recorded a decline of only 13.6 and 21.1 % compared to the control. Maximum MDA content (128.3 nmol/g Fwt) was found in non-treated seeds (Fig. 13b). Similarly, H₂O₂ content found in control (12.3 μ mol/g Fwt) seeds was significantly higher than the content in 1.6 % BNC (8.4 μ mol/g Fwt) treated seeds (Fig. 13a). Moreover, a decline of upto 31 % in H₂O₂ content was reported in BNCs-treated seeds (Fig. 13a).

3.2.5. Activity of antioxidant enzymes

The activities of key antioxidant enzymes superoxide dismutase (SOD) and catalase (CAT) were monitored to evaluate the seed response to the BNC treatments (Fig. 13). The results show that on BNCs application, the CAT activity was provoked compared to bulk and control. Moreover, the activity was enhanced by 51 % in 1.6 % BNC, which is higher than the bulk Zn and SA, showing an increase of only 14.3 and 7.5 % compared to non-treated seeds (Fig. 13d). Similarly, in the case of SOD the activity was significantly higher than the bulk- and non-treated seeds with a value of 2.33 unit/g Fwt in BNCs. BNCs treatment with 0.4 % showed an increase of 26.6 % in SOD activity compared to control seeds (Fig. 13c). Whereas, activity in bulk Zn and SA increased upto 5.1 and 11.9 %, respectively.

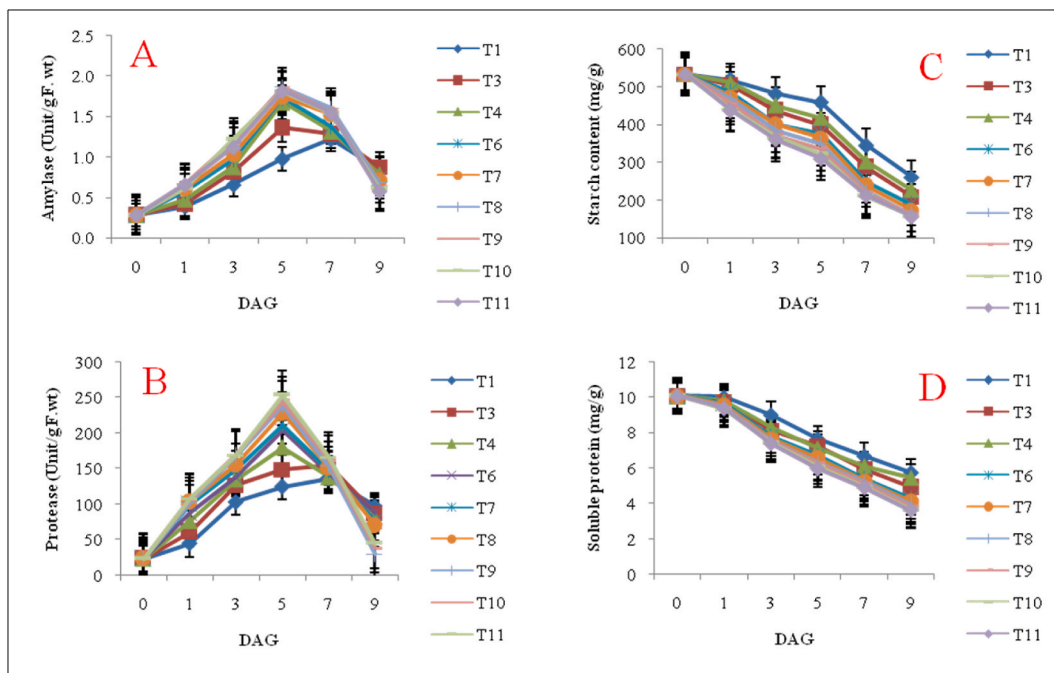


Fig: 11. Effect of nanopriming on seed reserve mobilizing enzyme α -Amylase (A) and protease (B), starch content (C), and soluble protein (D).

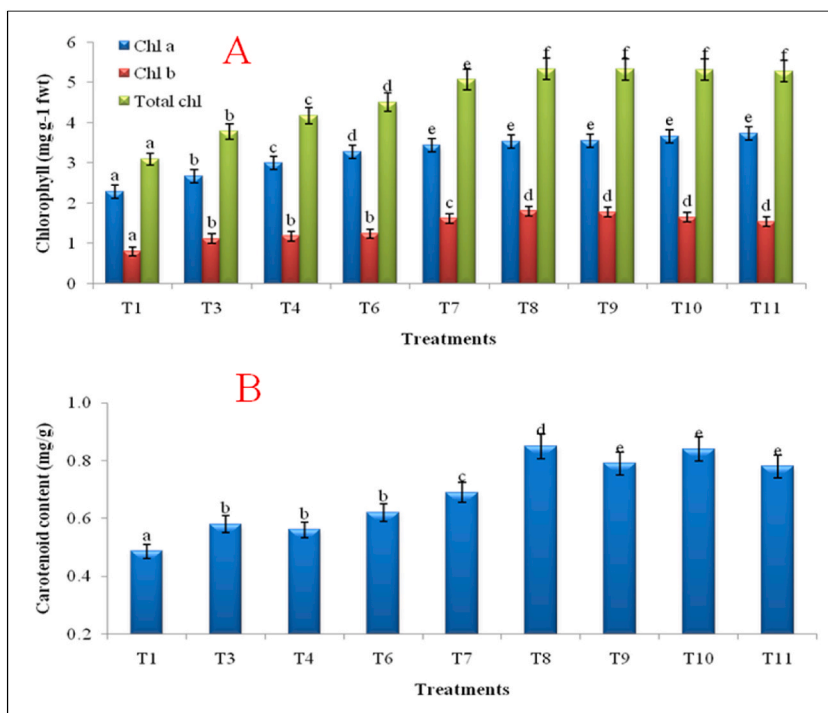


Fig: 12. Effect of nanopriming on chlorophyll A and B and total chlorophyll (A) and carotenoid content (B) in wheat.

4. Discussion

Zn-SA-chitosan BNCs developed and employed in the present study were monodispersed with a low PDI value (0.18 ± 0.04) and higher positive surface charge ($+25.2 \pm 2.4$ mV) with a mean size of 480 ± 6.0 nm (Fig. 3). Chitosan biopolymer was crafted into

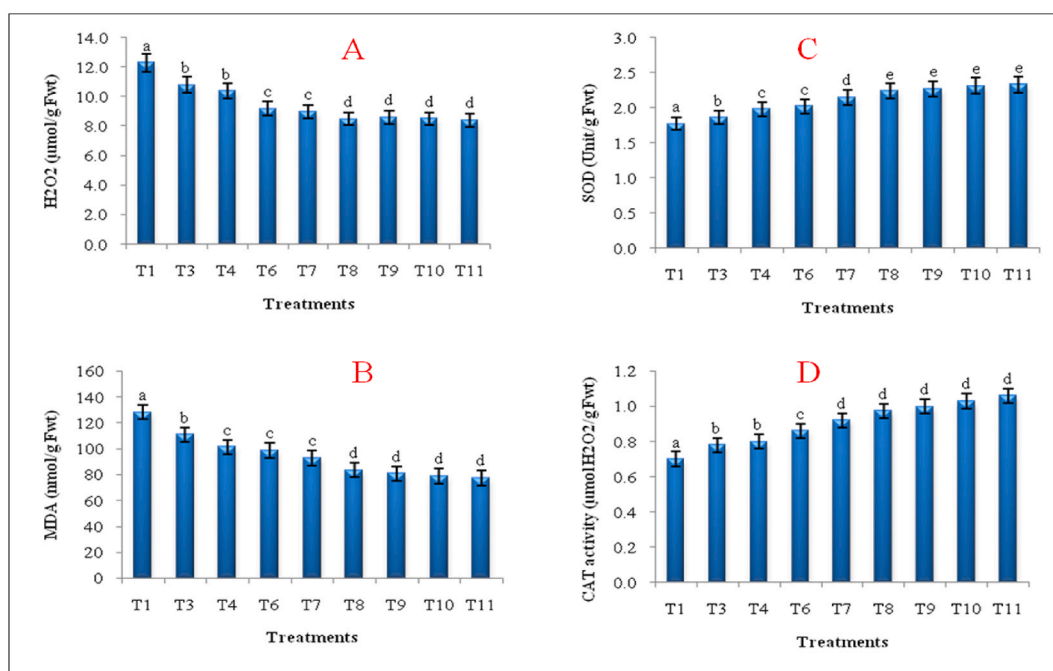


Fig. 13. - Effect of nanoprimering on stress indicators H₂O₂ (A) and MDA (B) and antioxidant enzymes SOD (C) and CAT (D) content in wheat seedlings at 15 DAG.

monodispersed spherical nanostructures by encapsulating Zn and SA during the process of cross-linking of linear biopolymer by TPP. The monodispersed NPs are crucial for their effortless influx to plant cells using cellular passages/and surface openings. A higher positive surface charge provides sufficient stability that abates aggregation and agglomeration in aqueous media. This charge is also necessary for its strict attraction with negatively charged plant cell/organelle membranes for greater responsiveness [23,45].

The porosity network in the developed BNCs visible in the TEM analysis demonstrates their spherical clumpy character (Fig. 4b). Additionally, SEM infers that the BNCs were spherical, porous and that the pores present are symmetrical and orchestrated too, which are essential for the proper co-encapsulation of Zn and SA and their subsequent slow-release (Fig. 4a). SEM-EDS spectrum verified the existence of C, P, O, and N and Zn deposition in the porous BNCs (Fig. 5). These SEM-EDS results concur with those of [46], who confirmed and proved the entrapment of Zn inside the nanoparticles. The chemical interfaces of Zn and SA with chitosan were evident from the FTIR study (Fig. 6), which agrees with earlier studies [33]. The presence of the relevant peaks further demonstrates that the produced BNCs are doped with Zn and SA (Fig. 6). Considering the interactions confirmed by FTIR, a theoretically possible structural ionic positioning in BNC having the backbone of chitosan cross-linked by TPP encapsulating Zn and SA is shown in Fig. 7. Another speculative morphology of Zn-SA-chitosan BNCs showing the blending of bulk Zn, SA, chitosan, and TPP to form a bionanoconjugate is hypothesized in Fig. 7.

BET (Brunauer Emmett Teller) analysis determines the physisorption features of the BNCs. Bulk chitosan has less surface area, pore volume, and pore radius than BNCs (Table 1). These results are consistent with earlier findings which subsequently guarantee the higher absorption and efficient entry of these BNCs in the seed and plant cells during imbibition and transpiration, respectively [47]. The surface area of nanoparticles is an important parameter as it is directly related to their reactivity, stability, and efficacy in various applications [48].

Encapsulation efficiency (EE) of Zn (78.4 %) and SA (58.9 %) in BNCs is significantly better than in prior studies [45,49]. Additionally, the synthesized Zn-SA chitosan BNCs exhibited exceptional loading capacity of the encapsulated constituents (Zn and SA), essential for their superior biological characteristics. Better EE of SA could be attributed to the strong inter- and intra-molecular interactions with the carrier polymer. Intermolecular interactions involve the hydroxyl and carboxylic acid moieties present in the SA molecule, which participated in hydrogen bonding and electrostatic linkages, respectively, with both the metal ions and the groups present in the chitosan polymer (Fig. 7). For SA, both the interactions may occur because the pKa of SA is 2.97. The pH of BNCs is considerably higher; as a result, SA can deprotonate and interact with the positive charges [50]. Deprotonation enables the electrostatic interactions between the active agent and the surface of the BNCs (thus representing positive zeta-potential). Moreover, the stronger interactions that could maintain the active agent trapped inside the BNCs include hydrogen bonds between the amino groups of chitosan polymer and the -COOH group of SA which can be an answer for extended release of ingredients (Fig. 6). Recent findings revealed that release profiles of the SA/chitosan NPs at 37 °C (fixed) at pH of 5.5 and 7.4 after 5 h was 18 and 35 %, respectively, whereas, after 22 h the release was found to increase up to 68 and 31 % respectively. Nanoparticles developed in previous findings reported that oxide nanoparticles could sustain maximum release for upto 530 min [51]. The difference in the release time of the two ingredients can be explained by the nature of the chemical interactions between the active agent and the polymers, the hydrophilicity

of the BNCs, and the closing of the polymeric network. The intricate process of nutrient release and seed uptake depends on various factors, mainly temperature and pH, responsible for the BNCs' uptake and post-uptake release in seedlings [25]. Zn and SA were found to be released from BNCs more quickly at lower pH than at neutral. This rapid release from BNCs is attributed to the protonation of the chitosan amino group at acidic pH. It is also predicted that the defined, symmetrical and porous network of the BNCs might have played a significant role in slow and sustained release of Zn and SA (Figs. 8–9). In contrast to the bulk application of Zn, SA, chitosan [52–54], and their sole nanoparticles [55], as described in earlier studies, the slow rate of nutrient release in the present study may supply nutrients over a prolonged duration that may have sustainable impacts on the crop.

The first-order release kinetics of the BNCs further determines the favourable results for release and retention rate constants of the encapsulated materials (Fig. 10). The release kinetics, or the rate and pattern of nutrient release, can have a significant impact on the effectiveness of these bionanoconjugates. The slow release of nutrients is an important factor in designing and applying bionanoconjugates [56]. A slow and sustained release of nutrients provides a continuous supply of essential elements to the plant, promoting healthy growth and reducing the need for frequent reapplication of fertilizers. This can also reduce the risk of nutrient toxicity and environmental pollution, as a slow release ensures a controlled and consistent supply of nutrients to the plant [57].

Strong seedling establishment is essential for obtaining decent crop produce since it boosts a plant's ability to withstand environmental challenges throughout the stages of growth. According to studies, seed priming with bulk chitosan promotes numerous genes associated with glucose metabolism in plants, increasing seedlings' vigour [58]. It is also observed that applying bulk and nano zinc individually improved seed germination, growth, and, eventually, yield [59]. Similarly, the sole application of SA has also been reported to establish wheat plants successfully [60]. Furthermore, prior studies frequently suggest that seed treatment with nano-materials improves seedling growth [36,61].

Table 2 demonstrates that seeds treated with BNCs have greater germination rates, coefficients of germination, and percentages of germination than untreated and bulk-treated seeds. Low germination rate leads to a reduced stand density, making it difficult for the crop to compete with weeds and leading to a lower rate of crop growth. A high germination rate ensures that the seedlings are healthy and vigorous, which results in a more uniform and robust crop with less stress pressure. The current analysis also revealed that BNCs considerably increased seed vigour (I and II) and seedling growth in the wheat genotype (WH-1124). Seed vigour indicates the seed's vitality and ability to produce a seedling with good root development, shoot growth, and overall health. Studies have shown that seed vigor positively correlates with crop yield and grain quality [62]. The BNCs also resulted in higher seedling length and fresh and dry weight than the control. It is reported that the larger the surface area higher the absorption of moisture and nutrients. Longer roots ensure a good supply of nutrients for better seedling growth and assist seedlings in thriving in the changing environmental/plant conditions [63]. It is hypothesized that the primed seeds' higher root-shoot length, seedling length, and fresh and dry weight may be attributable to their primed seeds' early and robust growth, which is the outcome of the prompt and efficient actions of reserve food mobilizing enzymes (Table 3). The BNCs significantly increased the α -amylase and protease activity (Fig. 11), which also correlated with the mobilization of reserve material (starch and protein) during seed germination (Fig. 11). It is suggested that chitosan nanoparticles could easily penetrate the cells due to their size, which results in enhanced bioactivities in the plant [64]. Similar results of improved germination by seed priming were obtained in barley, wheat, and maize when their seeds were treated with chitosan and SA nanoparticles [52,65,66]. Studies also evidenced that chitosan can stimulate root cell division by activating plant hormones such as auxin and cytokinin, which further contribute to the increased uptake of nutrients [67,68].

The amount of chlorophyll and carotenoid in a seedling is another crucial factor strongly associated with nitrogen content and photosynthesis [69]. In our findings, BNCs-treated seedlings had greater chlorophyll contents (Fig. 12). MDA and H_2O_2 , the markers of lipid peroxidation and oxidative stress, respectively, act as key indicators of cellular oxidative stress. High levels of MDA and H_2O_2 can damage cellular membranes, proteins and DNA, affecting the germination process. BNCs used in our study significantly reduced MDA and H_2O_2 during seedling development. The presence of SA in BNCs, which has a signalling function, might have played a key role here. This reduction is also credited to the corresponding increase in antioxidant enzymes, viz., SOD and CAT [70].

We also found it interesting that priming wheat seeds with greater Zn-SA chitosan BNCs concentrations (1.6 %) did not abate overall seedling growth, which could be attributed to the slow release of Zn and SA. Therefore, the gradual release of these active substances may have masked their sudden exposure to plant cells and avoided toxicity. Although the higher BNCs concentrations did not avert seed germination and growth, the treatments with concentrations above 0.4 % in seed priming primarily revealed non-significant increases in seed germination traits. The synergistic functions of SA and Zn in nutrient mobilization and seed germination may account for the significant rise in seedlings' potential for growth in the current study.

5. Conclusion

The developed BNCs were spherical, porous, monodisperse, stable, and had a slow-release feature. Seed priming with these BNCs for 14 h effectively increased seed germination potential. To augment and alter seed reserve mobilization potential in wheat, the Zn-SA-chitosan BNCs that own the release of Zn and SA in a leisurely manner are better than the solely applied nutrients. We also contend that the synthesized BNCs are made primarily of biodegradable and abundantly available biopolymer, making them environmentally friendly and cost-effective for crops with immense economic potential. Applying Zn-SA-chitosan BNCs to promote overall plant development under terminal heat and drought stress may be investigated.

Data availability statement

Data will be made available on request.

CRediT authorship contribution statement

Narender Mohan: Validation, Methodology, Investigation, Data curation, Conceptualization. **Ajay Pal:** Writing – review & editing, Visualization, Supervision, Formal analysis, Data curation, Conceptualization. **Vinod Saharan:** Validation, Investigation, Formal analysis, Data curation, Conceptualization. **Anuj Kumar:** Writing – review & editing, Validation, Resources, Formal analysis. **Rahul Vashishth:** Writing – review & editing, Visualization, Validation, Resources. **Sabina Evan Prince:** Writing – review & editing, Visualization, Validation, Supervision, Formal analysis.

Declaration of competing interest

The authors declare that they have no known competing financial interests or personal relationships that could have appeared to influence the work reported in this paper.

Acknowledgements

Chaudhary Charan Singh Haryana Agriculture University, Hisar, Haryana supported this work. We apologize to the authors whose work could not be cited in this review owing to space limitations.

References

- [1] M. Janni, et al., Molecular and genetic bases of heat stress responses in crop plants and breeding for increased resilience and productivity, *J. Exp. Bot.* 71 (13) (2020) 3780–3802, <https://doi.org/10.1093/jxb/eraa034>.
- [2] N. Mohan, et al., Acclimation response and management strategies to combat heat stress in wheat for sustainable agriculture: a state-of-the-art review, *Plant Sci.* (2023) 111834, <https://doi.org/10.1016/j.plantsci.2023.111834>.
- [3] M.A. Hassan, et al., Cold stress in wheat: plant acclimation responses and management strategies, *Front. Plant Sci.* 12 (July) (2021) 1–15, <https://doi.org/10.3389/fpls.2021.676884>.
- [4] W. Xiong, et al., Different uncertainty distribution between high and low latitudes in modelling warming impacts on wheat, *Nature Food* (2020), <https://doi.org/10.1038/s43016-019-0004-2>.
- [5] S. Chaudhry, G.P.S. Sidhu, Climate change regulated abiotic stress mechanisms in plants: a comprehensive review, *Plant Cell Rep.* (2021), <https://doi.org/10.1007/s00299-021-02759-5>.
- [6] A. Hossain, et al., Consequences and mitigation strategies of abiotic stresses in wheat (*Triticum aestivum* L.) under the changing climate, *Agronomy* 11 (2) (2021), <https://doi.org/10.3390/agronomy11020241>.
- [7] V. Marthandan, R. Geetha, K. Kumutha, V.G. Renganathan, A. Karthikeyan, J. Ramalingam, Seed priming: a feasible strategy to enhance drought tolerance in crop plants, *Int. J. Mol. Sci.* 21 (21) (2020) 1–23, <https://doi.org/10.3390/ijms21218258>.
- [8] M.M. Rahman, J. Crain, A. Haghhighattalab, R.P. Singh, J. Poland, Improving wheat yield prediction using secondary traits and high-density phenotyping under heat-stressed environments, *Front. Plant Sci.* 12 (2021), <https://doi.org/10.3389/fpls.2021.633651>.
- [9] M. Khan, et al., Trace Elements in Abiotic Stress Tolerance, 2018, https://doi.org/10.1007/978-981-10-9044-8_5.
- [10] S. Paparella, S.S. Araújo, G. Rossi, M. Wijayasinghe, D. Carbonera, A. Balestrazzi, Seed priming: state of the art and new perspectives, *Plant Cell Rep.* 34 (8) (2015) 1281–1293, <https://doi.org/10.1007/s00299-015-1784-y>.
- [11] F. Nadeem, M. Farooq, A. Ullah, A. Rehman, A. Nawaz, M. Naveed, Influence of Zn nutrition on the productivity, grain quality and grain biofortification of wheat under conventional and conservation rice–wheat cropping systems, *Arch. Agron Soil Sci.* (2020), <https://doi.org/10.1080/03650340.2019.1652273>.
- [12] P. Rai-Kalal, A. Jajoo, Priming with zinc oxide nanoparticles improve germination and photosynthetic performance in wheat, *Plant Physiol. Biochem.* 160 (January) (2021) 341–351, <https://doi.org/10.1016/j.plaphy.2021.01.032>.
- [13] A. Hameed, T. Farooq, A. Hameed, M.A. Sheikh, Sodium nitroprusside mediated priming memory invokes water-deficit stress acclimation in wheat plants through physio-biochemical alterations, *Plant Physiol. Biochem.* 160 (2021) 329–340, <https://doi.org/10.1016/j.plaphy.2021.01.037>.
- [14] A. Ignatenko, V. Talanova, N. Repkina, A. Titov, Exogenous salicylic acid treatment induces cold tolerance in wheat through promotion of antioxidant enzyme activity and proline accumulation, *Acta Physiol. Plant.* 41 (6) (2019), <https://doi.org/10.1007/s11738-019-2872-3>.
- [15] M. Calabi-Floody, et al., Smart fertilizers as a strategy for sustainable agriculture, in: *Advances in Agronomy*, vol. 147, Academic Press Inc., 2018, pp. 119–157, <https://doi.org/10.1016/bs.agron.2017.10.003>.
- [16] A. Ioannou, et al., Advanced nanomaterials in agriculture under a changing climate: the way to the future? *Environ. Exp. Bot.* 176 (Aug) (2020) <https://doi.org/10.1016/j.envexpbot.2020.104048>.
- [17] A. do Espírito Santo Pereira, H. Caixeta Oliveira, L. Fernandes Fraceto, C. Santaella, Nanotechnology potential in seed priming for sustainable agriculture, *Nanomaterials* 11 (2) (2021) 267.
- [18] R. Gobi, P. Ravichandiran, R. Shanker Babu, D.J. Yoo, “polymers biopolymer and synthetic polymer-based nanocomposites in wound dressing applications, A Review,” (2021), <https://doi.org/10.3390/polym13121962>.
- [19] R.V. Kumaraswamy, et al., Engineered chitosan based nanomaterials: bioactivities, mechanisms and perspectives in plant protection and growth, *Int. J. Biol. Macromol.* 113 (2018), <https://doi.org/10.1016/j.ijbiomac.2018.02.130>.
- [20] M. Azmana, S. Mahmood, A.R. Hilles, A. Rahman, M.A. Bin Arifin, S. Ahmed, A review on chitosan and chitosan-based bionanocomposites: promising material for combatting global issues and its applications, *Int. J. Biol. Macromol.* 185 (July) (2021) 832–848, <https://doi.org/10.1016/j.ijbiomac.2021.07.023>.
- [21] P.L. Kashyap, X. Xiang, P. Heiden, Chitosan nanoparticle based delivery systems for sustainable agriculture, in: *International Journal of Biological Macromolecules*, vol. 77, Elsevier, Jun. 01, 2015, pp. 36–51, <https://doi.org/10.1016/j.ijbiomac.2015.02.039>.
- [22] P. Deshpande, A. Dapkekar, M. Oak, K. Paknikar, J. Rajwade, Nanocarrier-mediated foliar zinc fertilization influences expression of metal homeostasis related genes in flag leaves and enhances gluten content in durum wheat, *PLoS One* 13 (1) (2018), <https://doi.org/10.1371/journal.pone.0191035>.
- [23] P.M. Kadam, et al., Physio-biochemical responses of wheat plant towards salicylic acid-chitosan nanoparticles, *Plant Physiol. Biochem.* 162 (2021) 699–705, <https://doi.org/10.1016/j.plaphy.2021.03.021>.
- [24] A. Kumar, et al., Slow-release Zn application through Zn-chitosan nanoparticles in wheat to intensify source activity and sink strength, *Plant Physiol. Biochem.* 168 (2021) 272–281, <https://doi.org/10.1016/j.plaphy.2021.10.013>.
- [25] J. Yu, D. Wang, N. Geetha, K.M. Khawar, S. Jogaiah, M. Mujtaba, Current trends and challenges in the synthesis and applications of chitosan-based nanocomposites for plants: a review, *Carbohydr. Polym.* 261 (Jun) (2021), <https://doi.org/10.1016/j.carbpol.2021.117904>.
- [26] S. Bandara, H. Du, L. Carson, D. Bradford, R. Kommalapati, Agricultural and biomedical applications of chitosan-based nanomaterials, *Nanomaterials* 10 (10) (2020) 1–31, <https://doi.org/10.3390/nano10101903>.
- [27] V. Saharan, A. Mehrotra, R. Khatik, P. Rawal, S.S. Sharma, A. Pal, Synthesis of chitosan based nanoparticles and their in vitro evaluation against phytopathogenic fungi, *Int. J. Biol. Macromol.* 62 (2013) 677–683, <https://doi.org/10.1016/j.ijbiomac.2013.10.012>.

- [28] A.E.S. Pereira, P.M. Silva, J.L. Oliveira, H.C. Oliveira, L.F. Fraceto, Chitosan nanoparticles as carrier systems for the plant growth hormone gibberellic acid, *Colloids Surf. B Biointerfaces* (2017), <https://doi.org/10.1016/j.colsurfb.2016.11.027>.
- [29] M. Shen, et al., The synthesis and characterization of monodispersed chitosan-coated Fe₃O₄ nanoparticles via a facile one-step solvothermal process for adsorption of bovine serum albumin, *Nanoscale Res. Lett.* 9 (1) (2014) 1–8, <https://doi.org/10.1186/1556-276X-9-296>.
- [30] C. Ryan, et al., Science and Technology of Advanced Materials Synthesis and characterisation of cross-linked chitosan composites functionalised with silver and gold nanoparticles for antimicrobial applications Synthesis and characterisation of cross-linked chitosan composites functionalised with silver and gold nanoparticles for antimicrobial applications, *Sci. Technol. Adv. Mater.* 18 (1) (2017) 528–540, <https://doi.org/10.1080/14686996.2017.1344929>.
- [31] S. Kumari, et al., Zinc-functionalized Thymol Nanoemulsion for Promoting Soybean Yield, 2019, <https://doi.org/10.1016/j.plaphy.2019.10.022>.
- [32] F.A. Razmi, N. Ngadi, S. Wong, I.M. Inuwa, L.A. Opotu, Kinetics, thermodynamics, isotherm and regeneration analysis of chitosan modified pandan adsorbent, *J. Clean. Prod.* 231 (2019) 98–109, <https://doi.org/10.1016/j.jclepro.2019.05.228>.
- [33] G. Sharma, et al., Chitosan nanofertilizer to foster source activity in maize, *Int. J. Biol. Macromol.* 145 (2020) 226–234, <https://doi.org/10.1016/j.ijbiomac.2019.12.155>.
- [34] J.S. Khokhar, et al., Novel sources of variation in grain Zinc (Zn) concentration in bread wheat germplasm derived from Watkins landraces, *PLoS One* 15 (2) (2020) e0229107, <https://doi.org/10.1371/journal.pone.0229107>.
- [35] F.P. Bonina, M.L. Giannossi, L. Medici, C. Puglia, V. Summa, F. Tateo, Adsorption of salicylic acid on bentonite and kaolin and release experiments, *Appl. Clay Sci.* 36 (1–3) (2007) 77–85, <https://doi.org/10.1016/j.clay.2006.07.008>.
- [36] V. Saharan, et al., Cu-chitosan nanoparticle mediated sustainable approach to enhance seedling growth in maize by mobilizing reserved food, *J. Agric. Food Chem.* 64 (31) (Aug. 2016) 6148–6155, <https://doi.org/10.1021/acs.jafc.6b02239>.
- [37] L. Shuster, R.H. Gifford, Changes in 3'-nucleotidase during the germination of wheat embryos, *Arch. Biochem. Biophys.* 96 (3) (Mar. 1962) 534–540, [https://doi.org/10.1016/0003-9861\(62\)90332-6](https://doi.org/10.1016/0003-9861(62)90332-6).
- [38] K.M. Clegg, The application of the anthrone reagent to the estimation of starch in cereals, *J. Sci. Food Agric.* (1956), <https://doi.org/10.1002/jsfa.2740070108>.
- [39] O.H. Lowry, N.J. Rosebrough, A.L. Farr, R.J. Randall, Protein measurement with the Folin phenol reagent, *J. Biol. Chem.* 193 (1) (1951) 265–275.
- [40] J.D. Hiscox, G.F. Israelstam, A method for the extraction of chlorophyll from leaf tissue without maceration, *Can. J. Bot.* 57 (1979) 1332–1334.
- [41] R.L. Heath, L. Packer, Photoperoxidation in isolated chloroplasts: I. Kinetics and stoichiometry of fatty acid peroxidation, *Arch. Biochem. Biophys.* 125 (1) (Apr. 1968) 189–198, [https://doi.org/10.1016/0003-9861\(68\)90654-1](https://doi.org/10.1016/0003-9861(68)90654-1).
- [42] A.K. Sinha, Colorimetric assay of catalase, *Anal. Biochem.* 47 (2) (Jun. 1972) 389–394, [https://doi.org/10.1016/0003-2697\(72\)90132-7](https://doi.org/10.1016/0003-2697(72)90132-7).
- [43] C. Beauchamp, I. Fridovich, Superoxide dismutase: improved assays and an assay applicable to acrylamide gels, *Anal. Biochem.* 44 (1) (Nov. 1971) 276–287, [https://doi.org/10.1016/0003-2697\(71\)90370-8](https://doi.org/10.1016/0003-2697(71)90370-8).
- [44] A.A. Abdul-Baki, J.D. Anderson, Vigor determination in soybean seed by multiple criteria, *Crop Sci.* 13 (1973) 630–633, <https://doi.org/10.2135/cropsci1973.0011183X001300060013x>.
- [45] R.V. Kumaraswamy, et al., Salicylic acid functionalized chitosan nanoparticle: a sustainable biostimulant for plant, *Int. J. Biol. Macromol.* 123 (2019) 59–69, <https://doi.org/10.1016/j.ijbiomac.2018.10.202>.
- [46] V. Saharan, et al., Synthesis and in vitro antifungal efficacy of Cu-chitosan nanoparticles against pathogenic fungi of tomato, *Int. J. Biol. Macromol.* 75 (2015) 346–353, <https://doi.org/10.1016/j.ijbiomac.2015.01.027>.
- [47] R.A. Elzamy, H.M. Mohamed, M.I. Mohamed, H.T. Zaky, D.R.K. Harding, N.G. Kandile, New sustainable chemically modified chitosan derivatives for different applications: synthesis and characterization, *Arab. J. Chem.* 14 (8) (2021), <https://doi.org/10.1016/j.arabjc.2021.103255>.
- [48] M.A. Kamal, S. Bibi, S.W. Bokhari, A.H. Siddique, T. Yasin, Synthesis and adsorptive characteristics of novel chitosan/graphene oxide nanocomposite for dye uptake, *React. Funct. Polym.* 110 (Jan. 2017) 21–29, <https://doi.org/10.1016/J.REACTFUNCTPOLYM.2016.11.002>.
- [49] R.C. Choudhary, et al., Zinc encapsulated chitosan nanoparticle to promote maize crop yield, *Int. J. Biol. Macromol.* 127 (2019) 126–135, <https://doi.org/10.1016/j.ijbiomac.2018.12.274>.
- [50] M. Hassanpour, et al., Salicylic acid-loaded chitosan nanoparticles (SA/CTS NPs) for breast cancer targeting: synthesis, characterization and controlled release kinetics, *J. Mol. Struct.* 1245 (2021), <https://doi.org/10.1016/j.molstruc.2021.131040>.
- [51] D. Mittal, G. Kaur, P. Singh, K. Yadav, Nanoparticle-based sustainable agriculture and food science: recent advances and future outlook, *Frontiers in Nanotechnology Nanotechnology* 2 (2020) 579954, <https://doi.org/10.3389/fnano.2020.579954>.
- [52] S.A. Alamri, M.H. Siddiqui, M.Y. Al-khaishani, H.M. Ali, Response of salicylic acid on seed germination and physio-biochemical changes of wheat under salt stress, *Acta Scientifica Agricultura* 2 (5) (2018) 36–42.
- [53] A. do E.S. Pereira, H.C. Oliveira, L.F. Fraceto, Polymeric nanoparticles as an alternative for application of gibberellic acid in sustainable agriculture: a field study, *Sci. Rep.* 9 (1) (Dec. 2019), <https://doi.org/10.1038/s41598-019-43494-y>.
- [54] S. Reis, I. Pavia, A. Carvalho, J. Moutinho-Pereira, C. Correia, J. Lima-Brito, Seed priming with iron and zinc in bread wheat: effects in germination, mitosis and grain yield, *Protoplasma* (2018), <https://doi.org/10.1007/s00709-018-1222-4>.
- [55] D. Prajapati, et al., Chitosan nanomaterials: a prelude of next-generation fertilizers; existing and future prospects, *Carbohydr. Polym.* 288 (Jul. 2022) 119356, <https://doi.org/10.1016/J.CARBPOL.2022.119356>.
- [56] S. Ojha, D. Singh, A. Sett, H. Chetia, D. Kabiraj, U. Bora, Nanotechnology in crop protection, in: *Nanomaterials in Plants, Algae, and Microorganisms*, vol. 1, Elsevier Inc., 2017, pp. 345–391, <https://doi.org/10.1016/B978-0-12-811487-2.00016-5>.
- [57] B. Beig, et al., Nanotechnology-based controlled release of sustainable fertilizers. A review, *Environ. Chem. Lett.* 20 (4) (2022) 2709–2726.
- [58] J. Kocięcka, D. Liberacki, The potential of using chitosan on cereal crops in the face of climate change, *Plants* 10 (6) (2021) 1160.
- [59] A. Hameed, A. Khalid, T. Ahmed, T. Farooq, Nano-priming with Zn-chitosan nanoparticles regulates biochemical attributes and boost antioxidant defence in wheat seeds. *Khanal, T. Ahmed, T. Farooq, Nano-priming with Zn-Chitosan Nanoparticles Regulates Biochemical Attributes and Boost Antioxidant Defence in Wheat Seeds*, 2020, pp. 207–221.
- [60] A. Mourya, S. Singh, Effect of Bio-fertilizers and plant growth regulators on growth and yield of Pearl millet, *Pennisetum glaucum* L., *Pharma Innov. J.* 11 (2022) 1791–1794.
- [61] A. Dapkekar, P. Deshpande, M.D. Oak, K.M. Paknikar, J.M. Rajwade, Zinc use efficiency is enhanced in wheat through nanofertilization, *Sci. Rep.* 8 (1) (2018), <https://doi.org/10.1038/s41598-018-25247-5>.
- [62] P. Rai-Kalal, R.S. Tomar, A. Jajoo, Seed nanoprimering by silicon oxide improves drought stress alleviation potential in wheat plants, *Funct. Plant Biol.* 48 (9) (2021) 905–915, <https://doi.org/10.1071/FP21079>.
- [63] S.M. de Sousa, et al., Tropical Bacillus strains inoculation enhances maize root surface area, dry weight, nutrient uptake and grain yield, *J. Plant Growth Regul.* 40 (2) (2021) 867–877.
- [64] C. An, et al., Nanomaterials and nanotechnology for the delivery of agrochemicals: strategies towards sustainable agriculture, *J. Nanobiotechnol.* 20 (1) (2022) 1–19, <https://doi.org/10.1186/s12951-021-01214-7>.
- [65] M. Farooq, T. Aziz, S.M.A. Basra, M.A. Cheema, H. Rehman, Chilling tolerance in hybrid maize induced by seed priming with salicylic acid, *J. Agron. Crop Sci.* 194 (2) (2008) 161–168, <https://doi.org/10.1111/j.1439-037X.2008.00300.x>.
- [66] T. Yadav, A. Kumar, R.K. Yadav, G. Yadav, R. Kumar, M. Kushwaha, Salicylic acid and thiourea mitigate the salinity and drought stress on physiological traits governing yield in pearl millet- wheat, *Saudi J. Biol. Sci.* 27 (8) (2020) 2010–2017, <https://doi.org/10.1016/j.sjbs.2020.06.030>.
- [67] H.-N. Maria, Stasinska-Jakubas and Barbara, Protective, Biostimulating, and Eliciting Effects of Chitosan and its Derivatives on Crop Plants, 2022.
- [68] K. Divya, M.S. Jisha, Chitosan nanoparticles preparation and applications, *Environ. Chem. Lett.* (2018), <https://doi.org/10.1007/s10311-017-0670-y>.
- [69] W. Mahboob, M.A. Khan, M.U. Shirazi, S. Faisal, Asma, S. Mumtaz, Seed priming induced high temperature tolerance in wheat by regulating germination metabolism and physio-biochemical properties, *Int. J. Agric. Biol.* 20 (9) (2018) 2140–2148, <https://doi.org/10.17957/IJAB/15.0747>.
- [70] T. Shah, et al., Seed priming with titanium dioxide nanoparticles enhances seed vigor, leaf water status, and antioxidant enzyme activities in maize (*Zea mays* L.) under salinity stress, *J. King Saud Univ. Sci.* 33 (1) (2021) 101207.